Construction and Building Materials 73 (2014) 645–651

Contents lists available at ScienceDirect

Construction and Building Materials

journal homepage: www.elsevier.com/locate/conbuildmat

Novel hybrid vacuum/triple glazing units with pressure equalisation design

Minxi Bao [a,b], Xiaogen Liu [c], Jian Yang [a,b,*], Yiwang Bao [c]

[a] School of Naval Architecture, Ocean and Civil Engineering, Shanghai Jiao Tong University, Shanghai 200240, PR China
[b] School of Civil Engineering, University of Birmingham, Edgbaston, Birmingham B15 2TT, UK[1]
[c] China Building Materials Academy, Beijing 51167946, PR China

HIGHLIGHTS

- A novel development of a hybrid vacuum/triple glazing system with a pressure equalisation design is reported.
- Negative pressure test was undertaken to examine the stresses and deformation generated in the new system.
- The maximum stresses and deflections were significantly reduced compared to the conventional design.
- This novel glazing system is safer than conventional vacuum glazing units.

ARTICLE INFO

Article history:
Received 17 May 2014
Received in revised form 3 October 2014
Accepted 9 October 2014

Keywords:
Vacuum glazing unit
Triple glazing
Hybrid glazing
Pressure equalisation
Pressure test
Energy efficient glazing

ABSTRACT

Vacuum glazing units (VGUs) are thought to be a type of glazing system with superior effective insulation performance. However, the differential pressure between the outside and the inner spaces and the supporting pillars create a high pre-existing stress field in the constituent glass during fabrication and hence make the units highly susceptible to breakage, even under small applied loads. In order to address this problem, a novel hybrid vacuum/triple glazing system with a pressure equalisation design has been devised and is reported in this paper. In this system, a VGU is enclosed by two glass panels to form a triple glazing unit system. This new design creates an equalised air pressure on both sides of the VGU hence subjects the VGU to no additional loads apart from the inherent fabrication stresses. This results in a high thermal and sound insulation as well as a more durable safety performance of the hybrid glazing component. Pressure tests were undertaken on the novel glazing system to confirm its reliability. Results show that under various loading levels, the stresses and deflections in the VGU of this novel glazing system always remain at a marginal level, and hence the likelihood of breakage for VGUs can be reduced significantly.

1. Introduction

Buildings are responsible for 40% of the total energy consumed in the EU [1]. While the insulating properties of opaque cladding or roofing components are relatively easy to enhance, windows and other glazing components are the least insulating parts and are often referred as heat sinks. Vacuum glazing units (VGUs), a newly emerging glazing technology, can potentially reduce heat loss through building windows or walls [2]. By utilizing the same mechanism as a thermos flask, an almost vacuum cavity is created to minimise the heat transfer by conduction and convection. By applying low-emission coatings, the heat loss caused by radiation can also be reduced. This glazing system can achieve a nominal *U*-value as low as 0.1 W/m^2 K [3–5]. However, relatively high fabrication costs and short lifetime have hindered the use of VGUs in the commercial sector [6]. Because of the low bulk strength of the annealed glass panels and the severe stress concentrations induced by the supporting pillars, VGUs exhibit low strength and are more susceptible to failure than conventional glazing units [7–9]. The bending strength of VGUs has been measured to be equal to only 40–50% of the strength of conventional monolithic glass of equivalent thickness [10]. The structural construction of a VGU is illustrated below in Fig. 1. The two glass panels in a VGU are separated by a narrow evacuated gap. A number of small metal or ceramic support pillars are placed between the two panels to

* Corresponding author. Tel.: +86 13917654726.
E-mail address: j.yang.3@bham.ac.uk (J. Yang).
[1] On leave. School of Civil Engineering, University of Birmingham, Edgbaston, Birmingham B15 2TT, UK.

http://dx.doi.org/10.1016/j.conbuildmat.2014.10.013
0950-0618/

maintain the evacuation cavity under atmospheric pressure. The differential pressure between the ambient pressure and that of the inner evacuated cavity, and the support pillars creates a high pre-existing stress field in the constituent glass during fabrication, and has therefore made the units highly susceptible to breakage, even under small applied loads.

In order to overcome this problem, two approaches are often considered: (1) to increase the strength of the glass panels that VGUs are made of; and (2) to reduce the mechanical loads and impact action on the VGUs in service. To date, most emphasis has been placed on the first approach. A common solution in line with the first concept is to develop a low-melting-point frit sealing technology [11–13] and then to introduce toughened glass instead of annealed glass. Hyde et al. [13] have successfully employed a type of edge seal with indium to realise the sealing process at a temperature of 200 °C or lower. However the available frit materials that can fulfil this purpose are very expensive, and therefore cannot be widely employed in practical applications. A US patent [14] offers a laser sealing technology that keeps the major part of the glass panels cool; however the construction process is complex and is unsuitable for mass production. The second concept entails a type of hybrid insulating/vacuum glazing unit fulfilling both purposes of load bearing and thermal insulation. It involves a glazing system comprising a VGU enclosed by two toughened glass panes [15]. The environmental load will be primarily applied on the outer panels, which is toughened glass in this design. External loads are mainly shared by both toughened glass panels with the inner air acting as the transferring medium. The air cavities separated by the inner VGU are linked, and thus the VGU will be subjected to an equal air pressure at both surfaces without causing any bending effects.

In this investigation, a novel hybrid vacuum/triple glazing system with a pressure equalisation design minimises the mechanical loads on the VGU without compromising their insulation performance, which yields a high safety performance. Windows are always subjected to long-term environmental actions like wind or snow, in the form of a uniformly distributed load (UDL). Uniform negative pressure tests were conducted in this study to imitate the equivalent environmental conditions. The experimental task was to verify that the new system met the design expectations, i.e. the VGU experiencing reduced stresses and deformation in service, and hence showing a higher safety performance.

2. Design concept of hybrid vacuum/triple glazing units (VGUs) with pressure equalisation

The conventional composite vacuum/triple glazing unit comprises two sheets of toughened monolithic glass panels and a VGU. The VGU is normally placed in the middle, dividing the air space into two, which can greatly enhance the thermal insulation performance while sharing the loads with the other two glass panels. The novel hybrid vacuum/triple glazing units have a similar configuration. The key difference is that this new design uses a small U-shaped pipe interlinking the two air spaces. The cross section of both glazing arrangements are illustrated in Fig. 2.

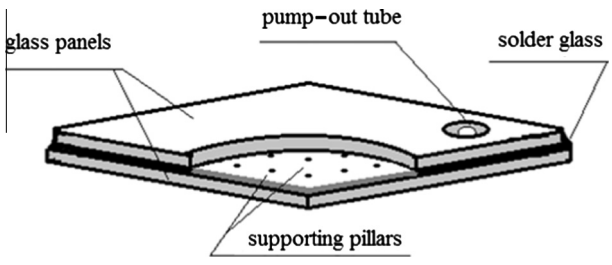

Fig. 1. Schematic diagram of vacuum glazing [9].

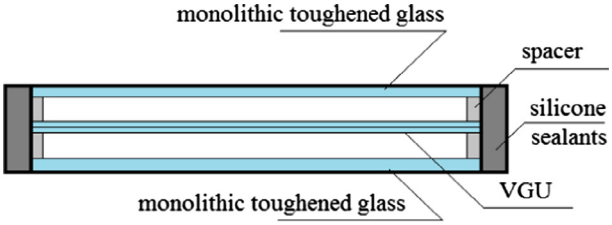

(a) Conventional composite VGU/triple glazing unit (Design I)

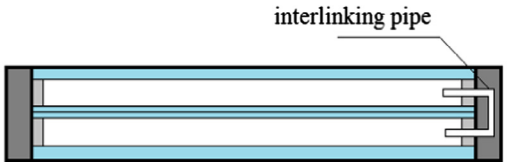

(b) Novel hybrid vacuum/triple glazing unit (Design II)

Fig. 2. Schematic diagram of two designs of VGU/triple glazing units.

In the conventional design (Design I), two air cavities are independently sealed. A uniform load applied to the outer glass panel will result in bending deformation in the glass, which subsequently reduces the volume of the air cavity. According to the Boyle's law for gas, the squeezed air will transfer the air pressure to the middle VGU and then to the inner glass panel. The VGU is subjected to additional differential pressure from both exposed surfaces, and experiences bending stresses, which are added to the inherent stresses caused by the difference between the atmospheric pressure and the evacuated cavity. A large load may render a failure of the VGU. However, in the pressure equalisation design (Design II) shown in Fig. 2(b), the U-shaped interlinking pipe provides a route to balance the pressure in the two air cavities separated by the VGU. When subjected to the environmental actions from wind load, the deformation of the receiving panel will drive air from the first cavity into the second one while maintaining equal pressures in both cavities. Therefore, the loads will be directly transferred to the inner panel, rather than acting upon the VGU.

3. Negative pressure test

In order to verify this novel design, a group of negative pressure test was undertaken. The test specimen was assembled with two toughened monolithic glass panels and a VGU, with a panel size of 1000 × 1000 mm. The thickness of the toughened monolithic glass panel is 6 mm and the selected VGU comprises two glass panels of 5 mm thickness. The panels were separated by 12 mm wide aluminium spacers. Silicone structural sealants were employed to glue the components together. Before sealing the edges, a set of strain gauge rosettes was applied to one surface of the VGU. The strain gauge rosettes consist of three gauges measuring the strains at angles of 0°, 45°, and 90°, respectively, as shown in Fig. 3. Two further sets of strain gauges were applied to the top and bottom surfaces of the toughened glass panels after the specimen was assembled. All strain gauges were glued at the centre of each panel, and the interlinking pipe was fixed at the edge of the square glass unit as shown in Fig. 4.

In order to compare the stresses and strains in both systems as shown in Fig. 2(a) and (b), an interlinking pipe with a switch valve was installed in the glazing system, as shown in Fig. 3. The pipe is made of polyvinyl chloride (PVC) and the internal radius is 2 mm.

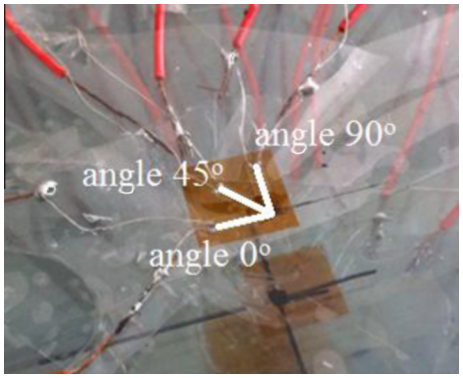

Fig. 3. Strain gauge rosette glued on glass surface.

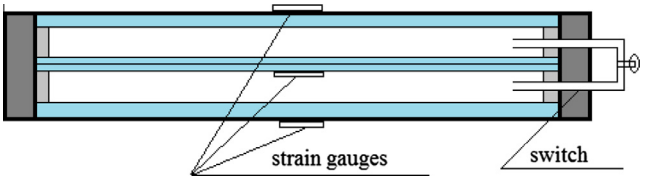

Fig. 4. Schematic diagram of the specimen with switchable pressure equalisation valve.

When the switch valve is off, the system is equivalent to the conventional composite glazing shown in Fig. 2(a) (Design I); whereas when the switch valve is on, the structure is equivalent to that in Design II, as shown in Fig. 2(b). Such a design allows the reuse of the test specimens during the comparison test. In order to have full curing of the silicone sealant, the sealed glazing units were placed in the laboratory for 14 days before the tests.

A negative pressure test device was set up as shown in Fig. 5. The test specimen was tightly glued onto a hermetic steel chamber using silicone sealants that can provide high air tightness within the chamber. A vacuum pump which could evacuate the inner air was connected to the chamber. A negative pressure dial gauge was installed in the hermetic chamber to indicate the pressure value. A strain gauge data acquisition system connected to the strain gauges was employed to record the strain changes on each glass panel, and the central deflection of the upper panel was measured by a precision laser displacement meter. The negative pressure tests were carried out three times for each glazing design by turning the switch valve on and off. The strains and the deflections were recorded at pressures ranging from 0.5 kPa to 3 kPa at 0.5 kPa intervals. The pressure versus time relationship is shown in Fig. 6. In each loading level, the pressure load remains constant for

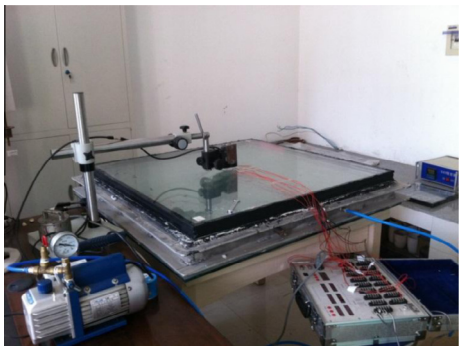

Fig. 5. Experimental devices for negative pressure test.

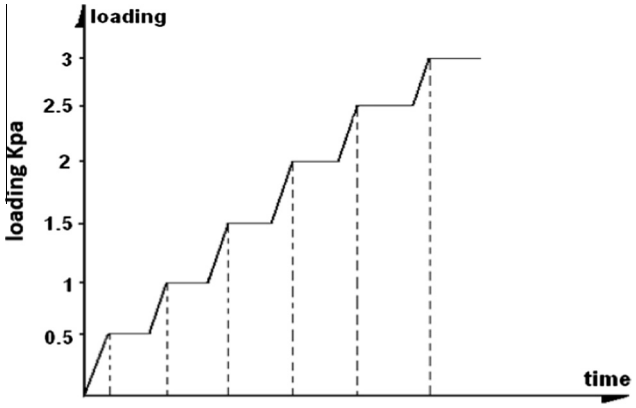

Fig. 6. Applied pressure process.

30 ± 5 s to allow the indicated strains in the glass panels to stay steady, and increases to next loading level within 10 s. The pressure tests were repeated three times for each type of glazing configuration.

4. Results and discussions

The strains in all three directions on the glass surfaces were measured at each pressure level using the strain gauges. At the centre point of the test unit, the two principal in-plane strains can be calculated by substituting the strains at 0°, 45°, and 90° into the equation below [16]:

$$\varepsilon_1 = \frac{\varepsilon_0 + \varepsilon_{90}}{2} + \sqrt{\left[\frac{(\varepsilon_0 - \varepsilon_{90})}{2}\right]^2 + \left[\frac{(\varepsilon_0 + \varepsilon_{90}) - 2\varepsilon_{45}}{2}\right]^2} \quad (1)$$

$$\varepsilon_2 = \frac{\varepsilon_0 + \varepsilon_{90}}{2} - \sqrt{\left[\frac{(\varepsilon_0 - \varepsilon_{90})}{2}\right]^2 + \left[\frac{(\varepsilon_0 + \varepsilon_{90}) - 2\varepsilon_{45}}{2}\right]^2} \quad (2)$$

The maximum principal stress can consequently be obtained [17]:

$$\sigma_{\max} = \frac{E}{1 - v^2}(\varepsilon_1 + v\varepsilon_2) \quad (3)$$

The glass is considered as a linear elastic, isotropic and homogeneous material. The maximum in-plane principal stress can be directly determined from the strains measured in three directions, by substituting Eqs. (1) and (2) into Eq. (3), which gives:

$$\sigma_{\max} = \frac{E}{2}\left\{\frac{\varepsilon_0 + \varepsilon_{90}}{1 - v} + \frac{1}{1 + v}\sqrt{(\varepsilon_0 - \varepsilon_{90})^2 + (\varepsilon_0 + \varepsilon_{90}) - [(\varepsilon_0 + \varepsilon_{90}) - 2\varepsilon_{45}]^2}\right\} \quad (4)$$

where E is Young's modulus and v is Poisson's ratio of the glass panel. For glass, Young's modulus is 72,000 MPa and Poisson's ratio is 0.22.

The average values of the maximum stresses on each panel were recorded and are presented in Table 1. The stress–pressure curves are plotted in Fig. 7, in order to present a clear comparison

Table 1
Stresses calculated by the measured strains.

Pressure (kPa)	0	0.5	1	1.5	2	2.5	3
Design I							
σ_{upper} (MPa)	0	0.76	1.71	2.75	3.32	3.92	4.41
σ_{VGU} (MPa)	0	1.27	2.53	3.70	4.79	5.74	6.84
σ_{lower} (MPa)	0	0.94	2.45	3.51	4.36	5.53	6.59
Design II							
σ_{upper} (MPa)	0	1.82	3.37	5.57	6.89	8.49	9.81
σ_{VGU} (MPa)	0	0.16	0.21	0.35	0.72	0.89	1.02
σ_{lower} (MPa)	0	1.92	3.83	6.03	7.31	9.26	11.45

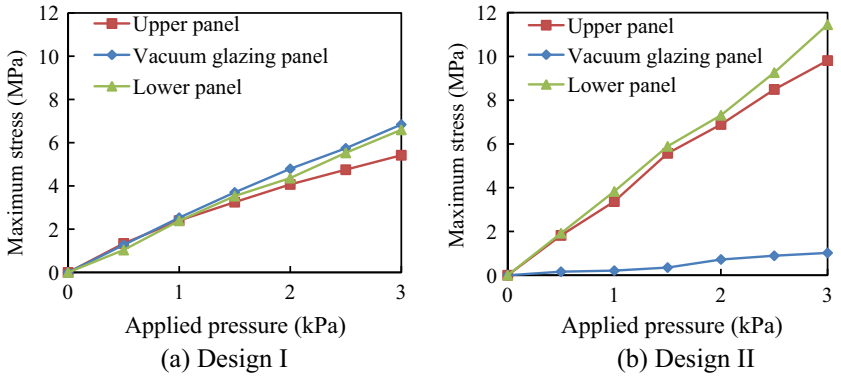

Fig. 7. Stresses measured for each glass panel.

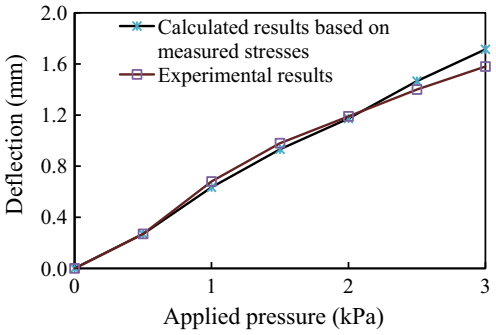

Fig. 8. Maximum deflections of the upper glass panel with increasing uniform pressure.

Table 2
Calculated deflections in two modes.

Pressure (kPa)	0	0.5	1	1.5	2	2.5	3
Mode I							
ω_{upper} (mm)	0	0.27	0.68	0.98	1.19	1.4	1.58
ω_{VGU} (mm)	0	0.34	0.68	0.99	1.28	1.54	1.84
ω_{lower} (mm)	0	0.34	0.88	1.26	1.56	1.98	2.36
Mode II							
ω_{upper} (mm)	0	0.68	1.26	2.08	2.57	3.17	3.64
ω_{VGU} (mm)	0	0.04	0.06	0.10	0.20	0.25	0.29
ω_{lower} (mm)	0	0.72	1.43	2.20	2.73	3.45	4.27

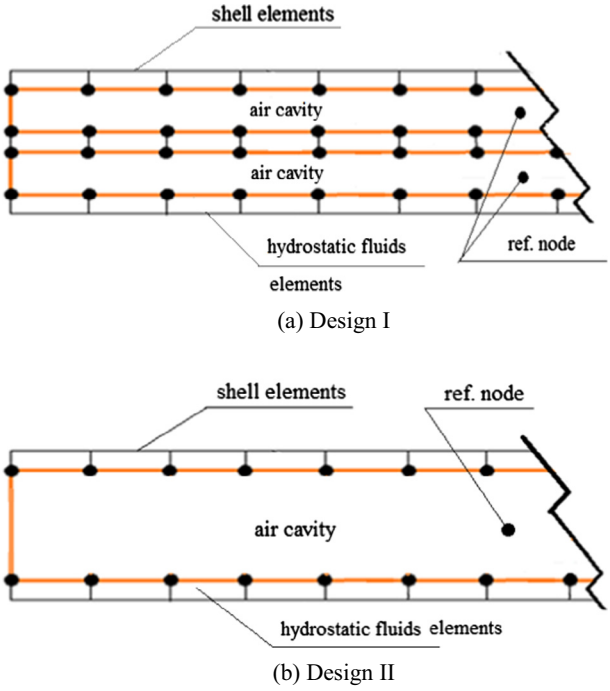

Fig. 10. Schematic diagrams of numerical models for both designs.

of the stresses developed in each panel. The maximum stresses are represented by their absolute values for the upper glass and the VGU, which is in compression on their upper surfaces.

The measured results of Design I indicate that when the lower panel is subjected to a uniform negative pressure, it will result in a dishing-type deformation and hence an expansion of the lower air space, which will subsequently lower its pressure and deform the VGU and the upper panel, causing a chain reaction. As expected, the stress in the lower panel is greater than that in the upper one by appropriately 30% to provide the load transfer via the air. The stresses developed in the glass panels of the VGU are more complicated. Both constituent panels of the VGU are sup-

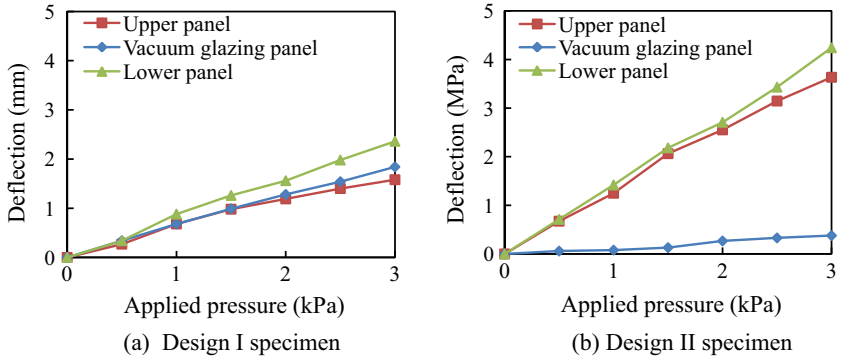

Fig. 9. Deflections of each glass panel in two glazing designs.

ported by a matrix of pillars. Under the test, the top panel is subjected to increased air pressure acting on its exposed surface, while it is supported at equally spaced discrete points. The reaction can then be transferred to the lower panel while maintaining the same cavity width facilitated by the pillars. The developed stresses therefore depend on the glass thickness and the pillar spacing. In the design case, the VGU can be treated as a monolithic glass panel with an effective thickness [9]. However, there is not yet any well-established model to calculate such effective thickness by allowing for the pillar arrangement.

Fig. 7(b) shows a different stress development in Design II. The stresses in both the upper and lower panels have been increased as compared to Design I. The middle VGU panel experiences only a small fraction of the stress that is induced in Design I. The results confirm that the stresses in the VGU have been successfully reduced by an average of 87.4% from Design I to Design II. Although the upper and lower panels have to withstand higher stresses in Design II, this can be easily overcome by using toughened glass.

The test also suggests that the pressure equilibrium between the two air cavities is not fully achieved under the prescribed loading rate. This type of lag effect can be easily altered by changing the size or number of interlinking pipes. Further research should be conducted to ensure that no high stresses will be induced during the application of the external loads that are of a dynamic nature, such as wind.

To further explore the load sharing/transferring behaviour of each glass panel, the maximum deflection of the glass panel is also examined. In this study, only the deflection of the upper panel was measured. As in the test, the glass panels behave in a linear elastic range, and the plate theory is used to calculate the deflections of the unmeasured panels by the strain records. This can be done by using the following equations [18]:

$$\sigma_{max} = \frac{\beta q b^2}{t^2} \tag{5}$$

$$\omega_{max} = \frac{\alpha q b^4}{E t^3} \tag{6}$$

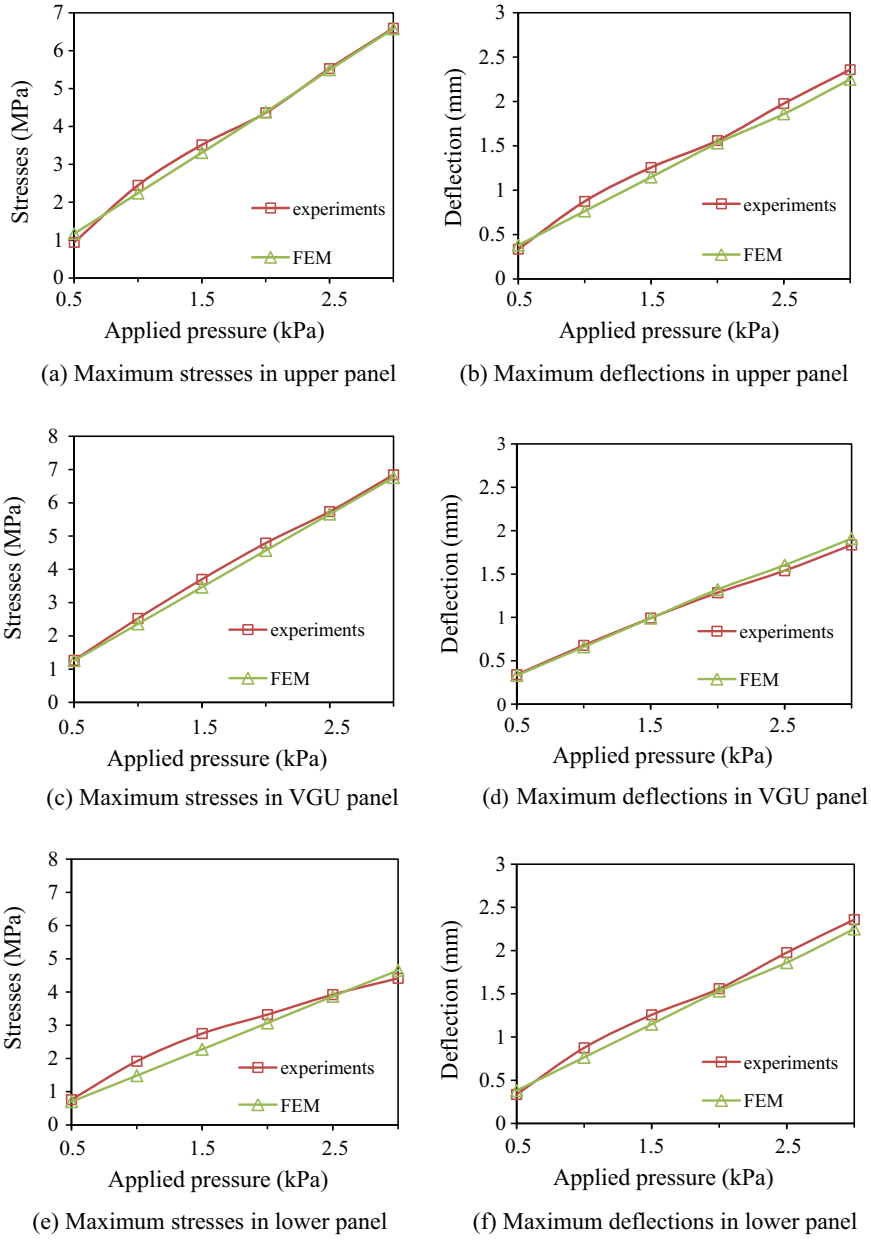

(a) Maximum stresses in upper panel
(b) Maximum deflections in upper panel
(c) Maximum stresses in VGU panel
(d) Maximum deflections in VGU panel
(e) Maximum stresses in lower panel
(f) Maximum deflections in lower panel

Fig. 11. Comparison of maximum stresses and deflections for Design I.

where b is the edge length of the plate, t is the thickness, E is Young's modulus, and α and β are the numerical constants that depend on the aspect ratio and material properties. When the aspect ratio of the plate equals 1, $\alpha = 0.0463$, and $\beta = 0.271$ for $v = 0.22$.

By substituting Eqs. (5) into (6), the maximum deflection can be obtained.

$$\omega_{max} = \frac{\alpha \sigma_{max} b^2}{\beta E t} \tag{7}$$

Eq. (7) is initially used to calculate the deflection of the upper panel, in order to provide a comparison with the recorded results. It can be seen that the results are very close and the proposed method by using Eq. (7) is validated as shown in Fig. 8.

The deflection of the inter-layer VGU and the lower toughened glass panel are calculated by Eq. (7). The results are shown in Table 2 and Fig. 9.

It should be noted that the thickness of the VGU used in Eq. (7) to calculate its bending deflection is an effective thickness rather than the actual thickness. It is estimated by substituting the measured stresses in the VGU into Eq. (5). The effective thickness of the VGU is found to be 8 mm by a trial and error method in the FE modelling.

As shown in Fig. 9(a), the central deflection of each glass panel decreases from the lower panel, to the VGU, and then to the upper panel. However, the deflection of the VGU in the pressure equilibrium hybrid glazing is almost negligible compared to the other two panels.

Both the stresses and the deflections in the VGU have been found to be reduced significantly. Therefore the new glazing design is able to reduce the loads on the VGU, which results in a significant reduction in the failure risk in the VGU. The hybrid vacuum/triple glazing with pressure equalisation design provides a solution to enhance the safety performance in VGUs without having to make them from toughened glass, which may still be technically or economically unviable.

5. FEM hydrostatic fluids analysis

A finite element model was also developed to simulate the two designs under test conditions. Hydrostatic fluid analysis method provided in the FEA software ABAQUS can be used to predict the mechanical response of a fluid filled or gas filled structure. Yuan et al. [19] employed this method to analyse the movement of vehicle air spring successfully. In the same way, this approach can also be used for the hermetic air cavities in the composite glazing unit. The trapped air can be assumed as the ideal gas, and modelled as a pneumatic fluid element that satisfies the ideal gas law described by Eq. (8) [20]:

$$\frac{\tilde{p}V}{\theta - \theta^z} = nR \tag{8}$$

where $\tilde{p}$ is the total fluid pressure, V is the air volume, θ is the temperature, θ^z is absolute zero on the temperature scale, n is the amount of a substance and R is an ideal gas constant. In the modelling exercise, the reference temperature, pressure and density are required to be entered as the input parameters. The trapped gas is simulated by the hydrostatic fluid element, which is a type of membrane elements sharing the same nodes with the cavity's interior surface. A reference node is set in the middle of the air cavity, connected to all hydrostatic fluid elements, by which the overall volume deformation and pressure variation can be calculated.

5.1. Model description

The hydrostatic fluid analysis method was employed to simulate the Design I sample with two isolated air cavities, and the Design II sample with two interlinking air cavities. The Design I

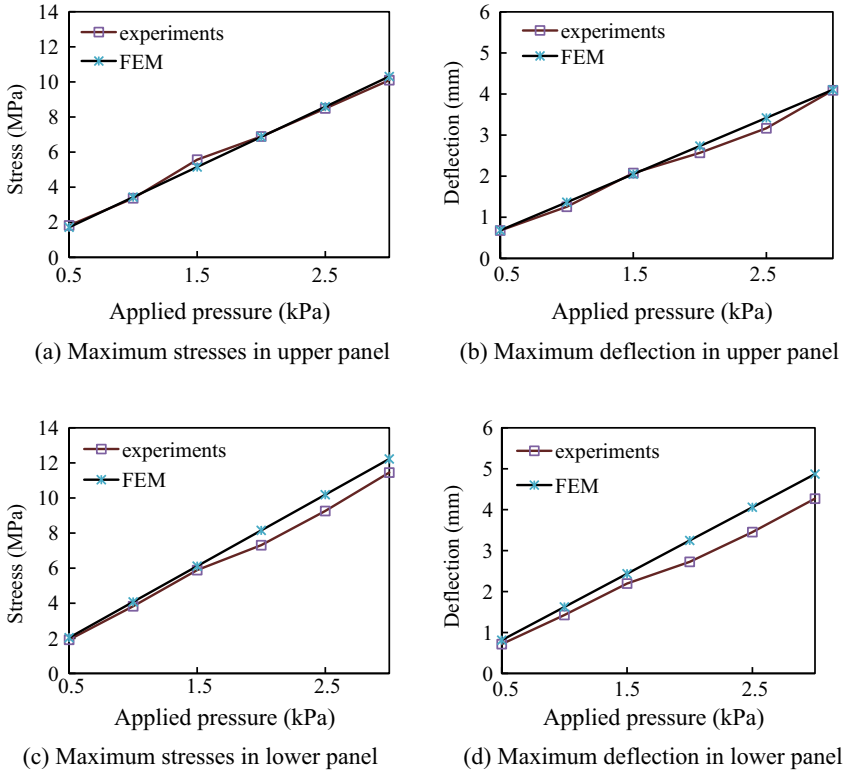

(a) Maximum stresses in upper panel (b) Maximum deflection in upper panel

(c) Maximum stresses in lower panel (d) Maximum deflection in lower panel

Fig. 12. Comparison of maximum stresses and deflections for Design II.

sample was modelled as a section of 6 mm + 8 mm + 6 mm triple glazing unit. In modelling Design II with pressure equalisation, it was assumed that the air movement between the two cavities had completed and hence the pressure was equalised. To simplify the modelling, an equivalent IGU with vanishing VGU was assumed. Numerical models reflected the actual size of the test specimen.

The numerical models were established as illustrated in Fig. 10. S4 shell elements were used to simulate the glass panels, and the hydrostatic fluid elements F3D4 were attached onto the glass panels. Although appearing as surface elements, the hydrostatic fluid elements were treated as volume elements by connecting to a reference node at the cavity centre, through which the volume change and internal pressure change can be calculated.

5.2. Results comparisons

A uniform negative pressure from 0.5 kPa to 3 kPa was applied to the lower glass panels of the models. The maximum stresses and deflections of each glass panel obtained from FEM modelling and the experiment are shown in Fig. 11.

As observed in Fig. 11, both sets of results are in good agreement. The average discrepancy is within 5%.

The maximum stresses and deflections of the upper and lower panels under increasing pressure loads in Design II are compared. The FEM results are compared with the experiment in Fig. 12.

As shown in Fig. 12(a) and (b), the experimental results in the upper panel agree well with the FEM modelling. A higher discrepancy is observed in the lower panel plotted in Fig. 12(c) and (d). The experimental results exhibit 6.34% lower stresses and 12.34% lower deflection than the theoretical results at the loading level, p = 3 kPa. The deviation results from the absence of the VGU panel in the FEM modelling, which in the test also experienced a minimal level of bending as shown in Fig. 7(b). It also implicates that the adopted load duration 30 s is not adequate to allow the system to reach fully equilibrium. The lagging issue can be alleviated by either increasing the pipe number or pipe size.

6. Conclusions

VGUs possess excellent thermal insulation capacity, but suffer a low strength due to pre-existing fabrication stresses. An innovative design has been proposed to minimise the applied loads acting on VGUs.

Pressure tests were carried out on a switchable glazing sample to verify the performance of the design intention. Compared with conventional composite glazing (Design I), the VGU adopted in the pressure equalisation hybrid glazing (Design II) experiences very low stresses and deflections. This novel design can incorporate conventional annealed-glass-based VGU products, which are currently widely available, with resultant products providing higher safety reliability.

A FEM hydrostatic fluids analysis was employed to simulate the bending behaviour of Designs I and II samples, which were subjected to negative pressure tests. In the simulation for Design I, FEM results are in good agreement with the experimental data, which provides a validation for the numerical model. In modelling Design II, FEM modelling yields slightly higher values in the maximum bending stresses and deflections. This arises from the assumptions used in the numerical modelling that the two interlinked air cavities are fully pressure-equalised. However, in the test, the inner VGU experienced a small level of bending action indicating the pressure equalisation had not yet been fully attained. Changing the size and number of interlinking pipes will adjust the time required for the pressure equalisation. Further research should be performed to identify the optimal interlinking pipe design to accommodate the wind load that is often of a dynamic nature.

The pressure equalisation system for the hybrid glazing has been verified as an effective structural/functional integration component for the building envelope, in which high thermal insulation and structural safety are both achieved for VGUs.

Acknowledgements

The authors would like to thank the support from China-UK International Collaboration Project (S2011ZR0397). The third author would also like to thank the support from the i) Project of National Natural Science Foundation of China (51378308); ii) Specialized Research Fund for the Doctoral Program of Higher Education, China (20130073120074); and iii) Innovation Program of Shanghai Municipal Education Commission (14ZZ027).

References

[1] Department for business innovation and skills. Estimating the amount of co_2 emissions that the construction industry can influence. London: BIS; 2010.
[2] Zoller A. Hollow pane of glass. German patent No. 387655; 1924.
[3] Manz H. On minimizing heat transport in architectural glazing. Renew Energy 2008;33(1):119–28.
[4] Tang J. Introduction of development and technique of vacuum glazing. In: Symposiums of Beijing synergy vacuum glazing technology Co Ltd; 2011. p. 1–6.
[5] Collins RE, Fischer-Cripps AC, Tang JZ. Transparent evacuated insulation. Sol. Energy 1992;49(5):333–50.
[6] Collins RE, Turner GM, Fischer-Cripps AC. Vacuum glazing-a new component for insulating windows. Build Environ 1995;30(4):459–92.
[7] Collins RE, Fischer-Cripps AC. Design of support pillar arrays in flat evacuated windows. Aust J Phys 1991;44(5):545–64.
[8] Wullschleger L, Manz H, Ghazi Wakili K. Finite element analysis of temperature-induced deflection of vacuum glazing. Constr Build Mater 2009;23(3):1378–88.
[9] Bao M, Yang J, Xu F. Optimisation of supporting pillars in vacuum glazing units. Eng Struct (submitted for publication).
[10] Liu XG. Safety evaluation and failure detection of glass curtain wall. PhD Thesis, 2009.
[11] Griffiths PW, M.D.L., et al. Fabrication of evacuated glazing at low temperature. Sol Energy 1998;63(4):243–9.
[12] Wang J et al. Stresses in vacuum glazing fabricated at low temperature. Sol Energy Mater Sol Cells 2007;91(4):290–303.
[13] Hyde TJ. Development of a novel low temperature edge seal for evacuated glazing. In: Sayigh AAM (editor). World renewable energy congress VI. University of Ulster, Newtownabbey: Northern Island, UK; 2000. p. 271–4.
[14] Benson DK. Laser sealed vacuum insulation windows. The United States of America as represented by the United States Department of Energy; 1987.
[15] Eames PC. Vacuum glazing: current performance and future prospects. Vacuum 2008;82(7):717–22.
[16] Bucciarelli LL. Engineering mechanics for structures. Dover Publications; 2009.
[17] Timoshenko SP, Goodier JN. Theory of elasticity. New York: McGraw-Hill; 1970.
[18] Young WC, Budynas RG. Roark's formula for stress and strain. McGraw-Hill; 2002.
[19] Yuan C, Zhou Kongkang, Wu Linqi, An D. Finite element method to analyze vehicle air spring. J Mech Eng 2009;45(6):42–6.
[20] Hibbitt K. ABAQUS/standard: user's manual. HKS co. Ltd.; 2007.